In-vivo pharmacokinetic & biodistribution studies

6. IN VIVO PHARMACOKINETIC AND BIODISTRIBUTION STUDIES

6.1 Introduction

Labeling of the PLGA and PBCA NP with radioisotopes was carried out by tagging with suitable gamma emitting radioisotope such as ^{99m}Tc. Two approaches for radiolabeling have been reported one is by attachment of the label to the polymer component prior to nanoparticle preparation and another way is to radiolabel the nanoparticle after manufacturing (Richardson et al., 1978). Radiolabeled nanoparticle have been successfully used for preclinical evaluation of pharmacokinetic parameters of nanocarrier delivery system as this can be administered to animals by different routes and its uptake in various organs can be estimated with time. Radiolabeled nanoparticle preparations have also been used successfully for imaging tumor, abscesses, ischemia and infracted region.

Nanoparticles can be labeled using various isotopes among them Technetium 99m (^{99m}Tc) was used widely due to its easy availability from Molybdenum-99 (^{99}Mo) as ^{99m}Tc generator and its favorable physical characteristics such as convenient short half life (6 hrs) and 140KeV gamma energy which is ideal for detection with current instruments. No particulate emission that decrease the radiation burden to the patient. Hence ^{99m}Tc has become the choice of isotope for nuclear medicine and currently ^{99m}Tc radiopharmaceuticals are available for imaging all major organs such as bone, liver, kidney, brain, heart etc. Various drug delivery systems such as nanoparticle, liposomes, gastro-retentive floating drug delivery systems, solid lipid dosage forms and colonic drug delivery systems have been currently evaluated using ^{99m}Tc (Arulsudar et al, 2003; Arulsudar et al, 2004; Subramanian et al, 2003; Reddy et al, 2004).

6.1.1 Radio Tagging Chemistry

Technetium, a transition metal element belongs to group VIIB of the periodic table. ^{99m}Tc can exist in eight oxidation namely 1^- to 7^+ among them, 7^+ and 4^+ are the most stable state and are represented in oxides, sulphides, halides and pertechnetate. The chemical form of ^{99m}Tc from Molybdenum generator is available as sodium pertechnetate (^{99m}Tc-$NaTCO_4$). The pertechnetate ion, $^{99m}TcO_4$- has the oxidation state 7^+ that resembles the permanganate ions MnO_4-. Pertechnetate is non-reactive and it is not possible to label any compound by direct addition of pertechnetate, so prior to labeling reduction of ^{99m}Tc from 7^+ state to lower oxidation is required (Saha 1993). Among the various reducing agents stannous ions in the form of chloride, tartarate is commonly used in acidic medium. The reduced ^{99m}Tc species are chemically reactive and combine with wide variety of ligands bearing chemical groups such as -COOH, -OH, $-NH_2$, and -SH as N,S, O act as good donor atoms for ^{99m}Tc. Other methods of labeling via HMPAO, or HYNIC are also reported in literature for liposomes.

6.1.2 Biodistribution and tumor targeting of Nanoparticles

The pharmacokinetics and tissue distribution of nanoparticle after parenteral administration are determined by a diversity of variables, including nanoparticle size and composition, stearic stabilization of the nanoparticle, presence of surface-grafted molecules, such as targeting devices and obviously, the organism and the health status of that particular organism. Upon injection, nanoparticles encounter anatomical barriers such as the endothelial lining of the vasculature and also of the blood-brain barrier, which will prevent access of the nanoparticles to extravascular sites. Only in organs such as the liver (see also later), spleen, bone marrow and under certain pathological conditions, such as occurring in solid tumors and at sites of infection or inflammation, the vascular endothelium may display enhanced permeability, allowing nanoparicles to extravasate (Ishida et al., 1999; Maruyama, 2000). The surface properties of particulate carriers greatly define their *in vivo* fate. The extent of blood clearance depend on the physicochemical properties of the particles, such as size, surface charge and surface hydrophobicity. The charge and the surface property carried by the colloidal particles can have an important role in determining the clearance and fate of the particles (Laverman et al., 1999).

Radiolabels, either encapsulated water-soluble compounds or bilayer-incorporated lipid labels, provide a sensitive and powerful tool to determine nanocarrier biodistribution. These markers provide a convenient way for a rapid and quantitative assessment of tissue distribution after parenteral administration of nanoparticles and produce reliable and reproducible data on tissue distribution both shortly after injection (1 - 4 h) and at longer times after injection (24 h). Apart from quantifying the radioactivity and estimating the percentage distribution in various organs it can also used to visualize the biodistribution of nanoparticle without sacrificing the animal by gamma scintigraphic imaging. Biodistribution of nanoparticle used can provide the information on localization of the carrier system in various organs which have been intended to target the specific site (Kamps and Scherphof, 2004).

Here we have studied the biodistribution of the developed PLGA and PBCA based nanoparticle delivery system in various organs after intravenous injection into mice and mice bearing bone tumor. We have compared the conventional, stealth and ZOL anchored nanoparticle, for targeting ability to bone and biodistribution in tumor induced swiss mice.

6.2 Radiolabeling of formulations and optimization

6.2.1 Materials

Stannous chloride dihydrate ($SnCl_2.2H_2O$) was purchased from Sigma Chemical Co.(St. Louis, MO), sodium pertechnetate, separated from molybdenom-99 (99m) by solvent extraction method, was provided by Regional Center for Radiopharmaceutical Division (Northern Region) Board of Radiation and Isotope Technology (BRIT, Delhi, India).

6.2.2 Radio-tagging and optimization

The formulations were radiolabeled using ^{99m}Tc by direct-labeling method (Eckelman et al., 1995; Babbar et al., 2000). Radiolabeled technetium in sodium pertechnetate was reduced in the acidic medium in the presence of stannous chloride.

For carrying out the radiolabelling of the formulations, the required volume of formulation was treated with stannous chloride in 0.1N hydrochloric acid and the pH was adjusted with sodium bicarbonate solution. Sterile sodium ^{99m}Tc-pertechnetate (35 to 40 mCi/mL) was added with continuous mixing such that the resultant solution has the required radioactivity for the animal studies. The mixture was incubated at 30°C ± 5°C for 10 minutes. The final required volume was made up with 0.9 %w/v sterile sodium chloride solution.

Generally technetium reduces in the presence of formulations, which enable the formulations tagged with technetium. In certain case, the previously reduced technetium is used for tagging of the formulations. The radiochemical purity of the formulations was determined using ascending instant thin layer chromatography (TLC). Silica gel-coated fiberglass sheets (Gelman Sciences Inc, Ann Arbor, MI) were used as stationary phase while dual solvent systems consisting of acetone and pyridine: acetic acid: water (3:5:1.5 v/v) were used as mobile phases (Saha, 1993; Saha, 2005). Since the free technetium is having R_f value of nearly 1 in mobile phase, the ratio of radioactivity in the top 1/3rd to lower 2/3rd of the ITLC plates were used as the index of the percentage labeled. The contaminants redued/ hydrolysed (^{99m}Tc) collectively were called as colloids which were identified by their lower R_f values in pyridine: acetic acid: water (3:5:1.5 v/v) mobile phase.

The effect of stannous chloride concentration on labeling was studied to achieve optimum labeling of the formulations and report in table 6.1. The in-vitro stability of radiolabeled formulations was evaluated in PBS pH 7.4 and mice serum by ascending ITLC (Garron et al., 1991) and tabulated in table 6.2. To evaluate stability and bonding strength of the labeled complex, the radio labeld formulations were challenged against various concentrations (2 and 4 mM) of Diethylene Triamine Penta acetic acid (DTPA). Since ^{99m}Tc- DTPA complex have higher R_f values in pyridine: acetic acid: water (3:5:1.5 v/v) mobile phase, where the radiolabeled formulations retained at point of application. The effect of different molar concentrations and percent transchelation on radiolabeled formulations was tabulated in table 6.3. Consequently, the optimized stable radiolabeled formulations were used for in vivo studies.

DTX loaded NP based formulations were radiolabeled by direct labeling method. The radiolabeling was optimized by consideration of two factors such as amount of stannous chloride and *in vitro* stability of the radiolabeled complex in saline as well as

in serum. The amount of stannous chloride should be kept minimum to avoid formation of hydro-colloids and 200 µgm found sufficient for effective labeling (table 6.1). The DTX, PLGA and PBCA based formulations were labeled successfully and their radio chemical purity/ labeling efficiency were found to be more than 90%. The stability studies of ^{99m}Tc-NP were carried out *in vitro* using normal saline and mice serum by ascending ITLC (Garron et al., 1991). *In vitro* stability of the complexes for 1h, 4h and 24h was assessed and the results were shown good stability as less than 10% dissociation of complex after 24 h (table 6.2). The bonding strength of ^{99m}Tc-NP was assessed by DTPA (Diethylene triamine penta acetic acid) challenging test (Babbar et al., 2000; Saha, 2005). The effect of different molar concentrations of DTPA on ^{99m}Tc-NP and percent transchelation were studied and less than 2 % transchelation observe after challenge with 2 and 4 mM DTPA (table 6.3).

Table 6.1: Effect of quantity of $SnCl_2$ on radiolabeling of DTX, PLGA NP and PBCA NP formulations

↓ Formulation	% Radiolabeled		
$SnCl_2$ (µgm) →	150	200	250
DTX	83.54 ± 3.75	98.23± 1.89	92.55 ± 4.14
PLGA NP	77.62 ± 3.85	99.11± 1.85	94.43 ± 3.48
PLGA-PEG NP	82.28 ± 4.11	98.68± 2.15	92.16 ± 3.16
PLGA-PEG-ZOL NP	81.64 ± 3.12	99.42± 1.89	88.69 ± 3.54
PBCA NP	80.83 ± 3.54	98.57± 1.85	91.13 ± 3.48
PBCA-PEG NP	82.42 ± 3.21	98.19 ± 2.15	92.48 ± 3.26
PBCA-PEG-ZOL NP	85.64 ± 3.19	98.21 ± 1.89	88.65 ± 3.54

Table 6.2: *In vitro* stability of radiolabeled DTX, PLGA NP and PBCA NP formulations

	↓ Formulation	% Radiolabeled		
	Time →	1 h	4 h	24 h
Saline	DTX	97.34 ± 3.64	95.52± 3.54	94.81 ± 2.34
	PLGA NP	98.52 ± 3.82	96.62± 3.62	95.73 ± 2.78
	PLGA-PEG NP	97.25 ± 3.71	96.17± 2.65	94.36 ± 2.76
	PLGA-PEG-ZOL NP	98.44 ± 3.42	97.02± 3.19	96.63 ± 3.24
	PBCA NP	97.73 ± 3.72	95.97± 2.82	94.23 ± 3.19
	PBCA-PEG NP	96.61 ± 3.63	95.39 ± 3.35	94.36 ± 3.27
	PBCA-PEG-ZOL NP	97.72 ± 3.29	95.81± 2.89	94.73 ± 3.17
Serum	DTX	96.91 ± 2.53	94.82± 1.92	94.15 ± 3.16
	PLGA NP	97.74 ± 2.65	95.71± 2.76	93.74 ± 2.52
	PLGA-PEG NP	96.78 ± 3.14	95.63± 2.75	94.04 ± 2.57
	PLGA-PEG-ZOL NP	97.87 ± 2.87	96.72± 2.74	94.72 ± 2.35

	PBCA NP	97.14 ± 2.62	95.79± 2.81	93.83 ± 2.73
	PBCA-PEG NP	96.22 ± 2.76	94.84 ± 2.16	93.68 ± 3.26
	PBCA-PEG-ZOL NP	97.06 ± 2.49	95.41 ± 2.63	92.74 ± 2.53

Table 6.3 Effect of DTPA on radiolabeling of DTX, PLGA NP and PBCA NP formulations

↓ Formulation	% Transchelation	
DTPA concentration →	2 mM	4 mM
DTX	1.23 ± 0.36	1.26 ± 0.44
PLGA NP	1.48 ± 0.52	1.64 ± 0.56
PLGA-PEG NP	1.76 ± 0.47	1.36 ± 0.43
PLGA-PEG-ZOL NP	1.69 ± 0.35	1.49 ± 0.59
PBCA NP	1.46 ± 0.34	1.32 ± 0.51
PBCA-PEG NP	1.82 ± 0.45	1.71 ± 0.47
PBCA-PEG-ZOL NP	1.63 ± 0.63	1.63 ± 0.73

6.3 Biodistribution Studies

The Social Justice and Empowerment Committee, Ministry of Government of India, approved all animal experiments were conducted for the purpose of control and supervision on animals and experiments. Swiss mice (aged 6 to 8 weeks), weighing between 20 to 25g, Swiss mice bearing desire size tumor, and without tumor were selected for the study. Three mice for each formulation per time point were used in this study. Radiolabeled complex of ^{99m}Tc-formulations of 100 µL of radiolabeled complex of ^{99m}Tc-solution was injected through tail vein of the mice. Blood was withdrawn by cardiac puncture after different time interval and the mice were sacrificed by cervical dislocation. Major organs (blood, heart, liver, spleen, kidney, lungs, tumor, intestine, stomach, tumor, tumor bearing bone, bone without tumor, tail, and brain) were isolated weighed and radioactivity present in each tissue/organ was measured using shielded well-type gamma scintillation counter. Radiopharmaceutical uptake per gram in each tissue/organ was calculated as a fraction of administered dose using equation:

$$\%\ Radioactivity\ per\ g\ of\ tissue = \frac{Counts\ in\ sample \times 100}{Wt\ of\ sample \times Total\ counts\ injected}$$

6.4 Results and Discussion

Biodistribution of ^{99m}Tc-NP following i.v. administration in swiss mice were performed and the radioactivity was estimated at predetermined time point for 1 h, 4 h and 24 h. The results obtained are shown in table 6.4 for PLGA NP formulations and

table 6.5 for PBCA NP formulations. The concentration of formulation in each organ/tissue/blood following i.v. injection of ^{99m}Tc-NP was shown in figure 6.1 for PLGA NP formulations and figure 6.2 for PBCA NP formulations in bar graph. The ratios of bio-distribution in liver, blood, tumor and bone were calculated and tabulated in table 6.6 for PLGA NP formulations and table 6.7 for PBCA NP formulations.

Table 6.4: Biodistribution of ^{99m}Tc labeled DTX and PLGA NPs and the radioactivity was measured after (a) 1 h, (b) 4 h and (c) 24 h post injection. The values represented here are the mean of three values with ± SEM. Radioactivity is expressed as percent of administered dose per gram of tissue or organ.

Table 6.4 (a)

% dose per gm of tissue after 1 h	DTX	PLGA NP	PLGA-PEG NP	PLGA-PEG-ZOL NP
Blood	7.3±0.7	7.8 ±0.8	10.2 ±1	9.8 ±0.95
Liver	3.3±0.5	5.6 ±0.6	3.4 ±0.4	3.2 ±0.4
Tumor	0.1±0.02	0.2 ±0.03	0.3 ±0.04	0.9 ±0.1
Bone without Tumor	0.1±0.1	0.1 ±0.03	0.1 ±0.02	0.3 ±0.04
Bone with tumor	0.1 ±0.2	0.2 ±0.04	0.2 ±0.03	1.5 ±0.18
Brain	2.1 ±0.3	0.4 ±0.05	0.3 ±0.04	0.2 ±0.03
Heart	2.3 ±0.3	2.4 ±0.3	2.2 ±0.3	2 ±0.23
Lung	0.4 ±0.06	0.3 ±0.04	0.3 ±0.03	0.2 ±0.03
Spleen	0.5 ±0.07	2.1 ±0.3	1.4 ±0.2	1.5 ±0.16
Kidney	2.3 ±0.4	0.3 ±0.05	0.3 ±0.04	0.4 ±0.05
Stomach	0.1 ±0.02	0.1 ±0.02	0.1 ±0.02	0.1 ±0.01
Intestine	0.2 ±0.03	0.1 ±0.02	0.1 ±0.02	0.1 ±0.02
Muscle	0.1 ±0.03	0.1±0.01	0.1 ±0.01	0.1 ±0.02

Table 6.4 (b)

% dose per gm of tissue after 4 h	DTX	PLGA NP	PLGA-PEG NP	PLGA-PEG-ZOL NP
Blood	4.6 ±0.6	6.5 ±0.82	8.3 ±1	8.1 ±0.94
Liver	2.1±0.4	5.3 ±0.6	2.1 ±0.4	2.3 ±0.4
Tumor	0.1 ±0.04	0.3 ±0.03	0.6 ±0.04	2.1 ±0.4
Bone without Tumor	--	0.1 ±0.02	0.1 ±0.02	1.1 ±0.2
Bone with tumor	--	0.1 ±0.03	0.1 ±0.03	3.2 ±0.5
Brain	1.6 ±0.25	0.3 ±0.04	0.2 ±0.03	0.2 ±0.04
Heart	1.4 ±0.23	2.1 ±0.3	1.9 ±0.3	1.6 ±0.2
Lung	0.3 ±0.05	0.2 ±0.04	0.2 ±0.04	0.2 ±0.03

Spleen	0.3 ±0.06	1.8 ±0.3	1 ±0.2	1.3 ±0.2
Kidney	1.8 ±0.4	0.2 ±0.04	0.2 ±0.05	0.3 ±0.04
Stomach	0.1 ±0.03	0.1 ±0.03	0.1 ±0.04	0.1 ±0.03
Intestine	0.1 ±0.032	0.1 ±0.025	0.2 ±0.03	0.1 ±0.02
Muscle	0.1 ±0.03	0.1 ±0.032	0.1 ±0.037	0.1 ±0.025

Table 6.4 (c)

% dose per gm of tissue after 24 h	DTX	PLGA NP	PLGA-PEG NP	PLGA-PEG-ZOL NP
Blood	1.3 ±0.16	4.2 ±0.5	6.3 ±0.8	6 ±0.9
Liver	0.5 ±0.08	3.7 ±0.43	1.1 ±0.23	1.4 ±0.2
Tumor	--	0.2 ±0.02	0.5 ±0.09	2.4 ±0.3
Bone without Tumor	--	--	0.08 ±0.02	1.1 ±0.3
Bone with tumor	--	0.1 ±0.03	0.07 ±0.09	3.3 ±0.5
Brain	0.6 ±0.08	0.2 ±0.04	0.2 ±0.04	0.1 ±0.02
Heart	0.5 ±0.07	1.2 ±0.3	1.3 ±0.23	1.1 ±0.2
Lung	0.1 ±0.03	0.1 ±0.03	0.1 ±0.03	0.1 ±0.03
Spleen	0.1 ±0.028	1.4 ±0.23	0.6 ±0.08	0.7 ±0.09
Kidney	0.4 ±0.06	0.1 ±0.03	0.1 ±0.03	0.2 ±0.04
Stomach	--	--	--	--
Intestine	--	--	--	--
Muscle	--	--	--	--

Table 6.5 Biodistribution of ^{99m}Tc labeled DTX and PBCA NPs and the radioactivity was measured after (a) 1 h, (b) 4 h and (c) 24 h post injection. The values represented here are the mean of three values with ± SEM. Radioactivity express as percent of administered dose per gram of tissue or organ.

Table 6.5 (a)

% dose per gm of tissue after 1 h	DTX	PBCA NP	PBCA-PEG NP	PBCA-PEG-ZOL NP
Blood	7.3 ±0.7	5.7 ±0.6	10.8 ±0.7	10.2 ±0.8
Liver	3.3 ±0.5	11.4 ±1.2	6.8 ±1	3 ±0.3
Tumor	0.1 ±0.02	0.2 ±0.05	0.2 ±0.04	0.35 ±0.1
Bone without Tumor	0.1 ±0.1	0.1 ±0.02	0.1 ±0.03	0.3 ±0.03
Bone with tumor	0.1 ±0.2	0.15 ±0.05	0.2 ±0.04	1.5 ±0.16
Brain	2.1 ±0.3	0.3 ±0.04	0.2 ±0.03	0.15 ±0.02

Heart	2.3 ±0.3	2.3 ±0.25	2.1 ±0.25	1.8 ±0.2
Lung	0.4 ±0.06	0.13 ±0.07	0.16 ±0.05	0.17 ±0.025
Spleen	0.4 ±0.07	4.1 ±0.8	3±0.65	1.4 ±0.13
Kidney	2.3 ±0.4	0.25 ±0.05	0.22 ±0.04	0.36 ±0.05
Stomach	0.1 ±0.02	0.08 ±0.018	0.1±0.02	0.09 ±0.01
Intestine	0.17 ±0.03	0.09 ±0.022	0.1 ±0.016	0.08 ±0.02
Muscle	0.1 ±0.03	0.1 ±0.01	0.1 ±0.01	0.1 ±0.016

Table 6.5 (b)

% dose per gm of tissue after 4 h	DTX	PBCA NP	PBCA-PEG NP	PBCA-PEG-ZOL NP
Blood	4.6 ±0.6	3.9 ±0.8	9.9 ±1	7.9 ±1.1
Liver	2.1 ±0.4	10.5 ±1.2	6.6 ±0.9	2.1 ±0.35
Tumor	0.1 ±0.04	0.4 ±0.06	0.6 ±0.08	1.2 ±0.35
Bone without Tumor	--	0. 1 ±0.03	0.15 ±0.025	1 ±0.18
Bone with tumor	--	0.1 ±0.02	0.15 ±0.02	3 ±0.4
Brain	1.6 ±0.25	0.2 ±0.03	0.25 ±0.04	0.15 ±0.05
Heart	1.4 ±0.23	2.3 ±0.24	1.6 ±0.27	1.4 ±0.21
Lung	0.3 ±0.05	0.09 ±0.03	0.11 ±0.04	0.15 ±0.035
Spleen	0.3 ±0.06	3.6 ±0.8	2.5 ±0.7	1.1 ±0.17
Kidney	1.8 ±0.4	0.23 ±0.03	0.18 ±0.04	0.3 ±0.05
Stomach	0.1 ±0.02	0.09 ±0.03	0.11 ±0.05	0.1 ±0.04
Intestine	0.09 ±0.028	0.1 ±0.022	0.19 ±0.032	0.08 ±0.018
Muscle	0.1 ±0.03	0.8±0.025	0.8 ±0.029	0.7 ±0.02

Table 6.5 (c)

% dose per gm of tissue after 24 h	DTX	PBCA NP	PBCA-PEG NP	PBCA-PEG-ZOL NP
Blood	1.3 ±0.16	1.1 ±0.6	6.2 ±0.7	6.1 ±0.9
Liver	0.5 ±0.08	3.6 ±1	3.2 ±0.7	1.24 ±0.15
Tumor	--	0.5 ±0.1	1.4 ±0.2	3.5 ±0.2
Bone without Tumor	--	--	0.07 ±0.02	0.9 ±0.25
Bone with tumor	--	0.08 ±0.02	0.08 ±0.06	3.1 ±0.4
Brain	0.6 ±0.08	0.17 ±0.03	0.19 ±0.03	0.9 ±0.015
Heart	0.5 ±0.07	1.1 ±0.25	1 ±0.2	1.3 ±0.25
Lung	0.1 ±0.03	0.05 ±0.01	0.07 ±0.02	0.1 ±0.02
Spleen	0.1 ±0.028	1.1 ±0.4	0.7 ±0.2	0.5 ±0.07
Kidney	0.4 ±0.05	0.09 ±0.03	0.11 ±0.04	0.18 ±0.05
Stomach	--	--	--	--

Intestine	--	--	--	--
Muscle	--	--	--	--

6.4.1 PLGA formulations

The prepared ^{99m}Tc-NPs complex was tested for labeling efficiency using TLC method. All formulations, DTX (98.2%), PLGA NP (99.1%), PLGA-PEG20 NP (98.7%) and PLGA-PEG-ZOL NP (99.4%) found high labeling efficacy as more than 98% activity found at base (lower 2/3rd). The biodistribution data reveals higher initial rapid uptake by liver, which was 5.6 % for PLGA NP and 11.4 % for PBCA NP after 1 h of post injection (Liu and Liu., 1996; Liu, 1997). Radioactivity of PEGylated PBCA NP and PLGA NP in liver after 1, 4 and 24 h was very less in comparison to nonPEGylated formulation as shown in table 6.4 and 6.5. The possible reason for higher retention of nonPEGylated NP in liver and spleen would be its hydrophobic surface which leads to RES uptake by liver and spleen after intravenous administration (Figure 6.1 and 6.2).

Figure 6.1 (a)

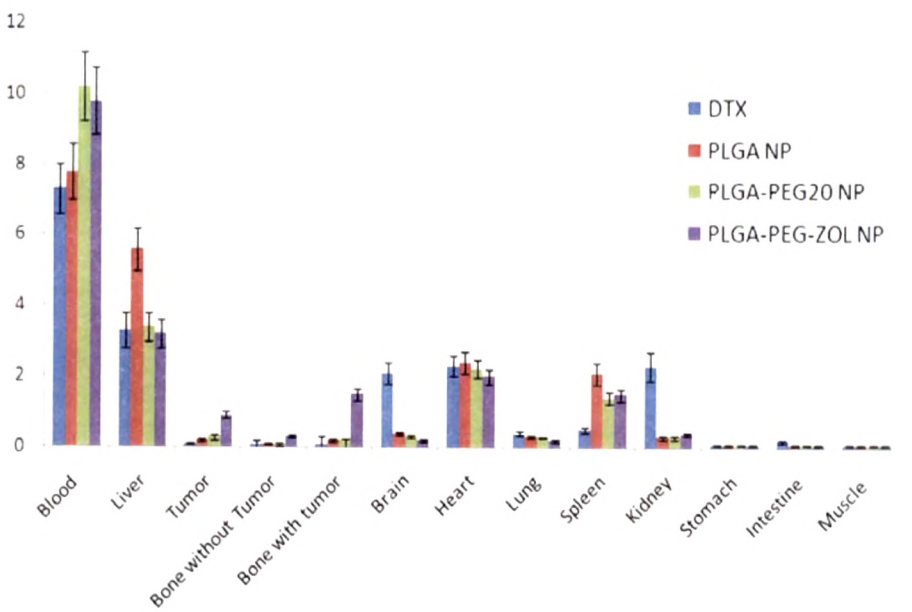

Figure 6.1 (b)

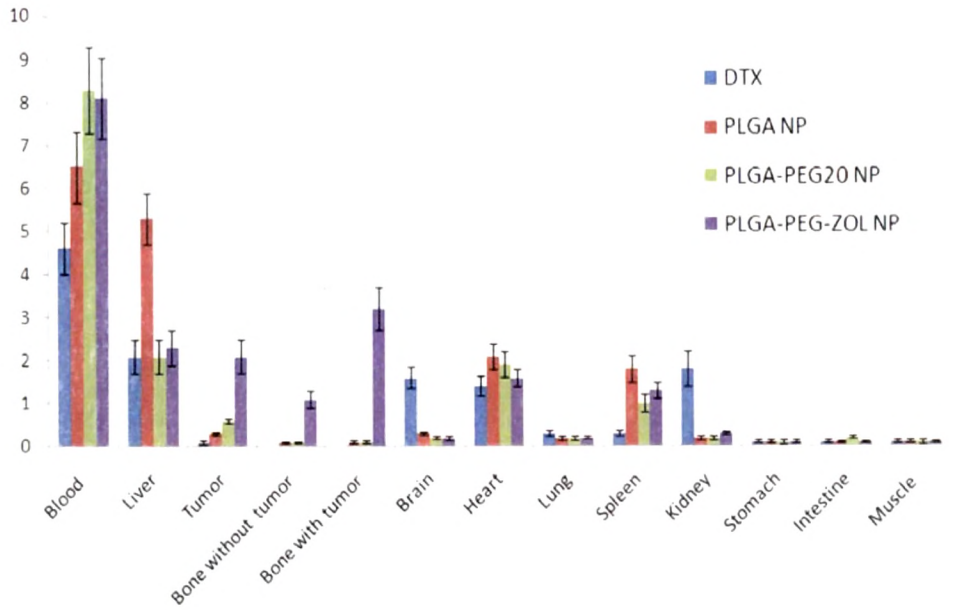

Figure 6.1 (c)

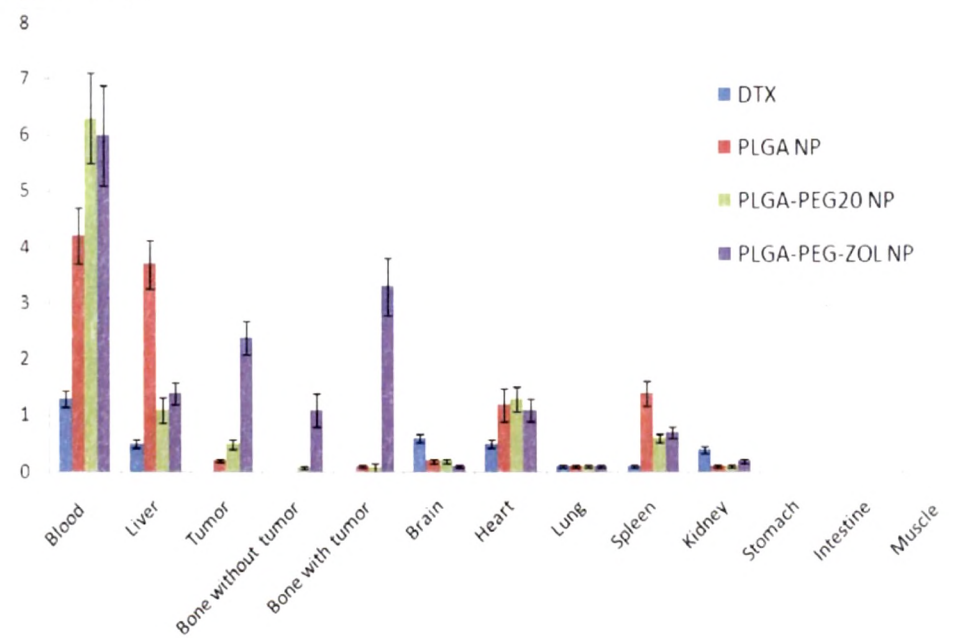

Figure 6.1: Mice were administered with ^{99m}Tc labeled DTX and PLGA NPs and the radioactivity was measured after (a) 1 h, (b) 4 h and (c) 24 h post injection. The

values represented here are the mean of three values with ± SEM. Radioactivity is expressed as percent of administered dose per gram of tissue or organ.

Table 6.6. Biodistribution of PLGA NP formulations by measuring radioactivity (^{99m}Tc-NP complex). Results represent ratio of radioactivity for various organ/tissue per gram.

	Formulation	Time		
		1 h	4 h	24 h
Blood to liver ratio	PLGA NP	1.39	1.23	1.14
	PLGA-PEG20 NP	3.00	3.95	5.73
Bone to Blood ratio	PLGA-PEG20 NP	0.020	0.012	0.011
	PLGA-PEG-ZOL NP	0.153	0.395	0.55
Tumor to Blood ratio	PLGA-PEG20 NP	0.029	0.072	0.079
	PLGA-PEG-ZOL NP	0.092	0.259	0.400
Tumor bearing bone to control bone	PLGA-PEG20 NP	2.0	1.0	0.9
	PLGA-PEG-ZOL NP	5.0	2.9	3.0

From the results of blood to liver NP distribution ratio, significant change could be observed in distribution of all NP formulations in blood and liver compartment which further increases with time (table 6.6 and 6.7). At 1 h time point, distribution ratio of PLGA-PEG20 NP is 2.15 fold higher than distribution ratio of PLGA NP (Table 6.6(a), fig. 6.1(a)). At 4 h time point, the distribution ratio was increased to 3.22 fold and even at 24 h time point it was increased considerably to 5.05 fold (Table 6.6(b), fig. 6.1(b)). Results clearly demonstrated that PLGA-PEG20 NP remains in blood for prolonged time in comparison to PLGA NP that retained more in liver. In case of ^{99m}Tc labeled PLGA NP and PBCA NP, liver and spleen accumulated a major portion of the administered radioactivity as they are the two major organs of reticulo-endothelial system (RES) which are known to accumulate and metabolize foreign particle (Semple et al., 1998; Monica et al., 2000).

Bone targeting affinity of PLGA-PEG-ZOL NP was determined from the ratio of NP distribution at tumor bearing bone in comparison to concentration in blood. The ratio of NP concentration in bone to blood was 50 fold higher with PLGA-PEG-ZOL NP than with PLGA-PEG NP after 24 h (Table 6.6(c), fig. 6.1(c)). At 1 h and 4 h time point, the distribution ratio was approximately 8 fold (780.6%) and 33 fold (3279%) accordingly (Table 6.6(a) & (b), fig. 6.1(a) & (b)). PLGA-PEG-ZOL NP distribution in tumor infected bone is also significantly high in comparison to normal bone. After 24 h the change in distribution was 3.5 fold higher (342.8%) in tumor bone than normal bone (table 6.6). The NP distribution at 1 h was 2.5 fold higher (250%) and at 4 h time point it was found to be 2.9 fold higher (290.0%) which show better

deposition of PLGA-PEG-ZOL NP at infected bone than normal bone. The tumor retention in comparison to blood for PLGA-PEG-ZOL NP was significantly higher (504%) than for PLGA-PEG20 NP after 24 h. At 1 h (312.2%) and 4 h (358.6 %) the retentions were also relatively high.

The outcomes showed that ZOL had more affinity toward infected bone than normal bone that enhanced NP retention at tumor site. Bone always cover with bone lining cells which prevent ZOL binding to bone to some extent, but when the active remodeling start in some disease such as osteoporosis, bone metastasis or bone tumor, the bone lining layer largely removed for active bone remodeling. ZOL have more affinity toward open bone remodeling site and get accumulated and stay for prolong time (Shea and Miller, 2005).

6.4.2 PBCA formulations

Stability of prepared ^{99m}Tc-PBCA NPs complex was tested for labeling efficiency using ITLC method. PBCA NP (98.57%), PBCA-PEG20 NP (98.19%) and PBCA-PEG-ZOL NP (98.21) found high labeling efficacy as more than 98% activity found at base (lower 2/3rd). From the results of blood to liver NP distribution ratio, significant change can be observed in distribution of both NPs formulation in blood and liver compartment which further increasing with time (Table 6.7). At 1 h time point, distribution ratio of PBCA-PEG20 NP is 3 fold high than distribution ratio of PBCA NP. At 4 h time point, the distribution ratio change to four fold and even at 24 h time point it change considerably to more than 6 fold. Results clearly show that PBCA-PEG20 NP remains in blood for prolong time in comparison to PBCA NP.

Figure 6.2 (a)

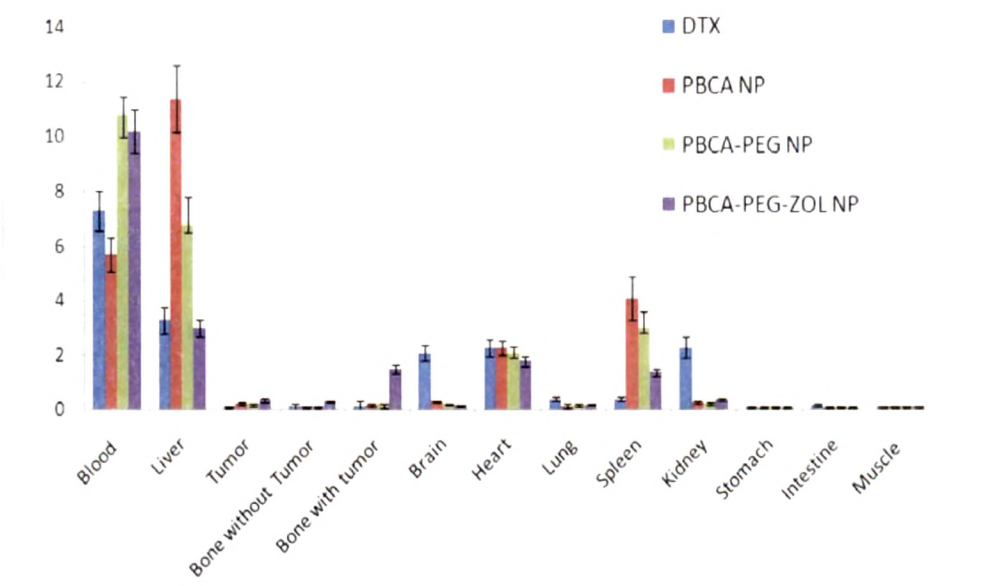

Figure 6.2 (b)

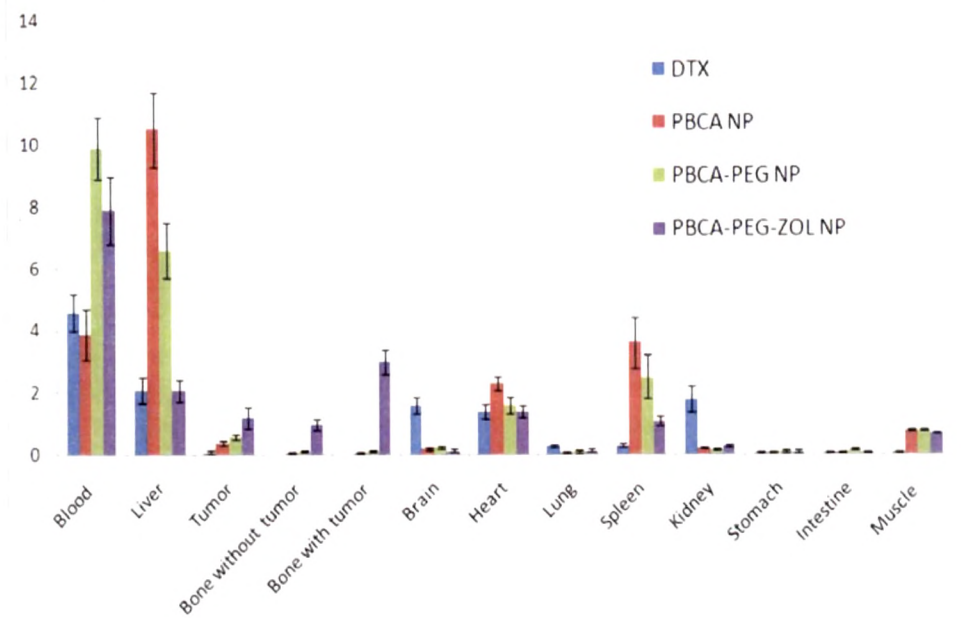

Figure6.2 (c)

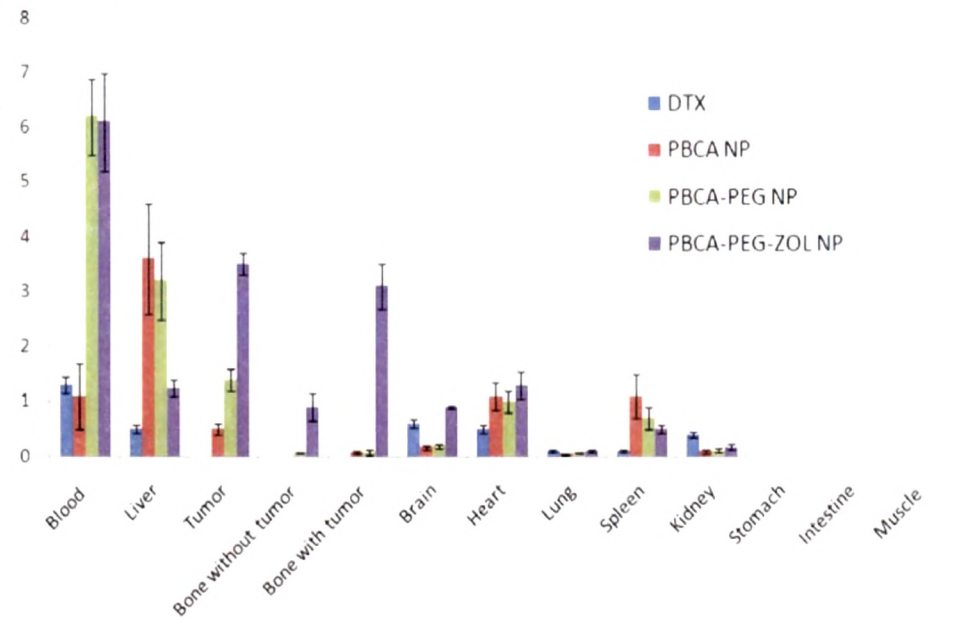

Figure 6.2: Mice were administered with ^{99m}Tc labeled DTX and PBCA NPs and the radioactivity was measured after (a) 1 h, (b) 4 h and (c) 24 h post injection. The

values represented here are the mean of three values with ± SEM. Radioactivity express as percent of administered dose per gram of tissue or organ.

Table 6.7. Biodistribution of PBCA formulations by measuring radioactivity (^{99m}Tc-NP complex). Results represent ratio of radioactivity for various organ/tissue per gram.

	Formulation	Time		
		1 h	4 h	24 h
Blood to liver ratio	PLGA NP	0.5	0.37	0.31
	PLGA-PEG20 NP	1.59	1.5	1.94
Tumor bearing Bone to Blood ratio	PBCA-PEG NP	0.02	0.02	0.01
	PBCA-PEG-ZOL NP	0.15	0.38	0.51
Tumor to Blood ratio	PBCA-PEG NP	0.02	0.06	0.23
	PBCA-PEG-ZOL NP	0.03	0.15	0.57
Tumor bearing bone to control bone	PBCA-PEG-ZOL NP	2.00	1.00	1.14
	PBCA-PEG-ZOL NP	5.00	3.00	3.44

Biodistribution of various PBCA NP formulations was evaluated for bone targeting affinity. For comparison of radio-distribution, results were also presented as ratio of distribution between two organs. The ratio of NP concentration in bone to blood was 39 fold higher for PBCA-PEG-ZOL NP than PBCA-PEG20 NP after 24 h (Table 6.7). At 1 h and 4 h time point, the distribution ratio was approximately 8 times (794.12%) and 25 fold higher (2506.33%) accordingly. PLGA-PEG-ZOL NP distribution in tumor infected bone is also significantly high in comparison to normal bone. After 24 h the change in distribution was 3 fold (301.39%) higher in tumor bone than normal bone. The NP distribution at 1 h (250.0%) and at 4 h (300.0%) was also show better deposition of PLGA-PEG-ZOL NP at infected bone than normal bone (Table 6.7). The tumor retention in comparison to blood for PBCA-PEG-ZOL NP is significantly high (254%) than for PBCA-PEG20 NP after 24 h. At 1 h (185%) and 4 h (251%) the retention are also relatively high. The results showed that ZOL had more affinity toward infected bone than normal bone because of ZOL enhanced NP retention at tumor site. Same time, PBCA-PEG-ZOL NP shown good bone and tumor uptake in comparison to PBCA-PEG20 NP.

Radiolabeling of drugs and nanocarrier systems were performed to study their organ distribution pattern and its fate *in vivo*. We have already reported wide success in the formation of stable radiolabeled complexes of drugs and nanocarriers and their use in pharmacokinetic studies (Arulsudar et al, 2003; Arulsudar et al, 2004; Subramanian et al, 2003; Reddy et al, 2004). The drug and NPs were radiolabeled with ^{99m}Tc and these radiolabeled complexes were intravenously administered to study blood clearance and biodistribution in mice model. *In vivo* animal study results showed clear

advantage of PBCA-PEG20 over other formulation in term of lower blood clearance, lower liver uptake and high blood concentration and prolong plasma half life. Lower up take in organ such as intestine and stomach confirmed *in vivo* stability of ^{99m}Tc-NP complex. *In vivo* results showed decrease in the concentration of PBCA NP in blood compartment with time and at the same time an increase in liver uptake, showing increased PBCA NP uptakes by liver macrophage. In comparison to PBCA NP, PBCA-PEG20 NP showed longer residence in blood compartment and comparatively less uptake by liver which displays its anti-phagocytic property. Tumor uptake also found significantly high in case of PBCA-PEG20 NP as a consequence of prolonged circulation resulted from more tumor retention by passive targeting through EPR effect. The ratio of blood to liver uptake results in *in-vivo* condition is also in compliance with *in vitro* phagocytic assay. The blood concentration of PBCA-PEG20 NP in blood remained significantly high even after 24 h in comparison to PBCA NP which indicates of long circulation half life of PBCA-PEG20 NP. ZOL has found predominat binding affinity with bone as a result more concentration of ZOL anchored formulation found at bone site. The tumor uptake also found significantly high which resulted as high local concentration of PBCA-PEG-ZOL NP and enhanced intracellular uptake by tumor cells.

Pharmacokinetic study for ZOL was carried out by Tianling Chen et al and reported that the 40% of ZOL was excreted after 24 h and 50% after 6 months. In report it was found that concentration of ZOL in bone was found more than 100 times of plasma C_{max} all the time point tested (Tianling Chen et al, 2002). Similar trend was also found in our study that the ZOL tagged NPs were found in very high concentration in bone than other organs, tissue or blood. The remarkable targeting efficiency resulted because of affinity of ZOL anchored NP toward infected bone site that make more NPs available for tumor retention and get internalized by endocytosis that enhanced in the presence of ZOL.

6.5 Conclusion

In vivo animal study using ^{99m}Tc radiolabeling was shown prolonged blood circulation half life, less liver uptake, higher retention of ZOL tagged NPs at bone site with enhanced tumor retention. The remarkable targeting efficiency was resulted because of affinity of ZOL anchored NP toward bone and tumor site. In this research we found enhanced targeting ability of PLGA-PEG-ZOL NPs and PBCA-PEG-ZOL NPs due to their strong affinity toward infected bone, EPR effect, prolong circulation half life as well as enhanced endocytosis. Thus, here we conclude that ZOL anchored PLGA NPs work as a novel tool for bone targeting and can be used to deliver therapeutics successfully in conditions such as bone tumor, bone metastasis or other bone diseases.

6.6 Reference

1. Arulsudar N, Subramanian N, Mishra P, Sharma RK, Murthy RSR. Preparation, characterization and biodistribution of 99mTc-labeled liposome encapsulated cyclosporine. J. Drug Targeting. 2003;11(3):187-196.
2. Subramanian N, Arulsudar N, Chuttani K, Mishra P, Sharma RK, Murthy RSR. Radiolabeling, biodistribution and tumor imaging of stealth liposomes containing methotrexate. J Alasbimn. 2003;6(22):Article 6.
3. Arulsudar N, Subramanian N, Mishra P, Chuttani K, Sharma RK, Murthy RSR. Preparation, characterization and biodistribution of Technetium-99m-labeled leuprolide acetate-loaded liposomes in Ehrlich Ascites tumor bearing mice. AAPS PharmSci. 2004;6:E5.
4. Reddy LH, Sharma RK, Chuttani K, Mishra AK, Murthy RSR. Etoposide-incorporated tripalmitin nanoparticles with different surface charge: formulation, characterization, radiolabeling, and biodistribution studies. AAPS J. 2004;6(3):55-64.
1. Babbar AK, Singh AK, Goel HC, Chauhan UPS, Sharma RK. Evaluation of ^{99m}Tc labeled Photosan-3, a heamatoporphyrin derivative, as a potential radiopharmaceutical for tumor scintigraphy. Nucl Med Biol 2000;27:419–426.
2. Eckelman WC. Radiolabeling with technetium-99m to study high-capacity and low-capacity biochemical systems. Eur. J. Nucl. Med.1995;22:249-263.
3. Garron JY, Moinereau M, Pasqualini R, Saccavini JC. Direct 99mTc labeling of monoclonal antibodies: radiolabeling and in-vitro stability. Int J Rad Appl Intru 1991;18:695-703.
4. Ishida O, Maruyama K, Sasaki K, Iwatsuru M. Size-dependent extravasation and interstitial localization of polyethyleneglycol liposomes in solid tumor-bearing mice. Int. J. Pharm. 1999;190:49-56.
5. Kamps AAM, Scherphof GL. Biodistribution and Uptake of Liposomes *in vivo*. Methods in Enzymology 2004;387:257-26.
6. Laverman P, Boermana OC, Wim JG, et al., Liposomes for scintigraphic detection of infection and inflammation, Adv. Drug Deliv. Rev. 1999;37:225-235.
7. Liu D. Biological factors involved in blood clearance of liposomes by liver. Adv. Drug Deliv. Rev. 1997;24:201-213.
8. Liu F, Liu D. Serum independent liposome uptake by mouse liver. Biochim. Biophys. Acta 1996;1278:5-11.
9. Maruyama K. *In vivo* targeting by liposomes. Biol. Pharm. Bull. 2000; 23: 791-799.
10. Monica CD, Valerie B, Elias F, et al., Improvement of *in vivo* stability of phosphodiester oligonucleotide using anionic liposomes in mice. Life Sciences 2000;67:1625-1637.

11. Richardson VJ, Jeyasingh K, Jewkes RF et al., Possible tumor localization of 99m Technetium labeled liposomes: effects of lipid composition, charge, and liposome size. J. Nucl. Med. 1978;19:1049-1054.
12. Saha GB. Fundamentals of Nuclear Pharmacy, 5th edition, New York: Springer-Verlag; 2005.
13. Saha GB. Methods of Radiolabeling. Saha GB. Physics and Radiobiology of Nuclear Medicine. Springer; New York: 1993;100-106.
14. Semple SC, Chonn A, Cullis PR. Interactions of liposomes and lipid-based carrier systems with blood proteins: Relation to clearance behavior *in vivo*. Adv. Drug Deliv. Rev. 1998;32:3-17.
15. Theobald AE. Theory and practice. In: Sampson C, Editor. Text book of radiopharmacy. New York, NY: Gorden and Breach.1990;127-128.
16. J.E. Shea, S.C. Miller, Skeletal function and structure: Implications for tissue-targeted therapeutics, Adv. Drug Delivery Rev. 57 (7) (2005) 945– 957.
17. T. Chen, J. Berenson, R. Vescio, R. Swift, A. Gilchick, S. Goodin, P. LoRusso, P. Ma, C. Ravera, F. Deckert, H. Schran, J. Seaman, A. Skerjanec, Pharmacokinetics and pharmacodynamics of zoledronic acid in cancer patients with bone metastases, J. Clin. Pharmacol. 42 (11) (2002) 1228–1236.